Explicit inclusion of electronic correlation effects in molecular dynamics

Jean-Pierre Julien, Joel D. Kress, and Jian-Xin Zhu

Phys. Rev. B **96**, 035111 — Published 7 July 2017

DOI: 10.1103/PhysRevB.96.035111

Explicit inclusion of electronic correlation effects in molecular dynamics

Jean-Pierre Julien,[1,2] Joel D. Kress,[2] and Jian-Xin Zhu[2,3]

[1] *CNRS/Université de Grenoble Alpes-Institut Néel, France*
[2] *Theoretical Division, Los Alamos National Laboratory, Los Alamos, New Mexico 87545*
[3] *Center for Integrated Nanotechnologies, Los Alamos National Laboratory, Los Alamos, New Mexico 87545*

(Dated: May 2, 2017)

We design a quantum molecular dynamics method for strongly correlated electron metals. The strong electronic correlation effects are treated within a real-space version of the Gutzwiller variational approximation (GA), which is suitable for the inhomogeneity inherent in the process of quantum molecular dynamics (MD) simulations. We also propose an efficient algorithm based on the second-moment approximation to the electronic density of states for the search of the optimal variation parameters, from which the renormalized interatomic MD potentials are fully determined. By considering a minimal one-correlated-orbital Anderson model with parameterized spatial dependence of tight-binding hopping integrals, this fast GA-MD method is benchmarked with that using exact diagonalization to solve the GA variational parameters. The efficiency and accuracy are illustrated. We have demonstrated the effect of temperature coupled with electronic correlation on structural properties simulated with MD. This novel method will open up an unprecedented opportunity enabling large-scale quantum MD simulations of strongly correlated electronic materials.

I. INTRODUCTION

Electronic correlation effects in materials such as transition metal oxides, give rise to emergent phenomena including Mott insulating state, magnetism, heavy fermion, and unconventional superconductivity. These phenomena defy the description of the density functional theory (DFT) within local density approximation (LDA), which has been successful in describing electronic and structural properties of good metals and several semiconductors. Other discrepancies show up for materials like elemental actinide solids. For instance, the experimentally measured equilibrium volume of δ-plutonium is 25% larger than the one given by the DFT-LDA approach, the greatest deviation known between experiment and theoretical value for this theory. The inadequacy of the DFT-LDA method for strongly correlated electron materials can be partly cured by including a direct treatment of quantum fluctuation effects by such quantum many-body approaches like the dynamical mean-field theory (DMFT).[1,2] Together with its success in describing key physical observables in many strongly correlated electron materials, however, the LDA+DMFT is computationally expensive and in practice limited to solid state systems with high crystalline symmetry, making it time consuming to describe the structural relaxation problems. The combination of LDA with the Gutzwiller variational method[3,4] has proved successful in providing an alternative but fast approach to the strongly correlated electron metals.[5]

We note that the energies and stability of various crystalline structures, and the structure of disordered liquids, of simple and d-band metals can be calculated by *ab initio* DFT methods alone and/or coupled with Molecular Dynamics (MD).[6] Computational requirements limit the application of DFT MD simulations to thin film surface slabs, and to a few interacting defects in the bulk, containing at most 300 to 400 atoms. Faster methods based on empirical fitting of electron density or tight-binding parameters, such as the Embedded Atom Method[7] and Second Moment Approximation,[8] respectively, are routinely employed in MD simulations consisting of thousands of atoms and more. Due to reasons outlined above, standard *ab initio* DFT methods are not suitable for strongly correlated electron metals. Therefore, MD simulations of strongly correlated electron metals, such as Pu, are limited to empirical methods,[9,10] where the quantum nature of the electronic degrees of freedom are not explicitly considered. As an initial step in the direction to include quantum effects in MD simulations of strongly correlated electron metals, we propose to combine the computationally efficiency of the GA method with MD.

The strategy seems to be straightforward in principle. However, practical applications to realistic systems present challenges. On the one hand, for an explicit treatment of strong electronic correlation effects, the *ab initio* method requires a definition of local correlated orbitals. On the other hand, for the MD, forces should be calculated on the fly. The aim of this work is to present a generic framework of the GA-MD method, together with a path forward for improving the computational speed of the GA optimization procedure. We propose the construction of such parameterizations as presented in the tight-binding electronic structure method, and the use of the semi-empirical second moment approximation of electronic density of states for the calculation of local kinetic energy. The latter will significantly speed up the minimization procedure in the Gutzwiller variational method for the electronic structure, opening up the possibility of MD simulations to strongly correlated electronic materials.

The outline of the paper is as follows. In Sec. II, we give a detailed description of the density matrix formulation of the Gutzwiller approximation. It has the advantage of being applicable to crystals, as well as topologically and/or chemically disordered and impurity systems.[5,15]

In Sec. III, we derive an approximate but analytical solution to the optimization equations in the GA, where a high quality fitted solution on the whole range of physical interest is provided, and propose the second moment approach to the electronic density of states for the calculation of kinetic energy parameters. In Sec. IV, the formulation of force on individual atoms is presented. In Sec. V, this efficient GA-MD method is demonstrated in a minimal Anderson model for heavy fermion systems based on tight-binding hopping integrals. A concluding summary is given in Sec. VI.

II. DENSITY MATRIX FORMULATION OF GUTZWILLER METHOD

A. Renormalization of hopping integrals

First, we review the Gutzwiller method briefly for which we closely follow Ref. 5 but here we specifically include the topological disorder, i.e., during a typical MD process, no symmetry remains and all atoms are inequivalent. Among numerous theoretical approaches, the Gutzwiller method provides a transparent physical interpretation in terms of the atomic configurations of a given site. Originally, it was applied to the one-band Hubbard model Hamiltonian:[11]

$$H = H_{kin} + H_{int} \ , \tag{1}$$

with

$$H_{kin} = \sum_{i \neq j, \sigma} t_{ij} c^{\dagger}_{i\sigma} c_{j\sigma} \ , \tag{2}$$

and

$$H_{int} = U \sum_{i} n_{i\uparrow} n_{i\downarrow} \ . \tag{3}$$

The Hamiltonian contains a kinetic part H_{kin} with a hopping integral t_{ij} from site j to i, and an interaction part with a local Coulomb repulsion U for electrons on the same site. $c^{\dagger}_{i\sigma}$ ($c_{i\sigma}$) is the creation (annihilation) operator of an electron at site i with up or down spin σ. $n_{i\sigma} = c^{\dagger}_{i\sigma} c_{i\sigma}$ measures the number (0 or 1) of electron at site i with spin σ. The Hamiltonian, Eq. (1), contains the key ingredients for correlated up and down spin electrons on a lattice: the competition between delocalization of electrons by hopping and their localization by the interaction. It is one of the most widely used models to study the electronic correlations in solids.

In the absence of the interaction U, the ground state is characterized by the Slater determinant comprising the Hartree-like wave functions (HWF) of the uncorrelated electrons, $|\psi_0\rangle$. When U is switched on, the weight of the doubly occupied sites will be reduced because of the cost of an additional energy U per site. Accordingly, the trial Gutzwiller wave function (GWF) $|\psi_G\rangle$ is built from the HWF $|\psi_0\rangle$:

$$|\psi_G\rangle = g^D |\psi_0\rangle \ . \tag{4}$$

The role of g^D is to reduce the weight of the configurations with doubly occupied sites, where $D = \sum_i n_{i\uparrow} n_{i\downarrow}$ measures the number of double occupations and g (< 1) is a variational parameter. This method corrects the mean-field (Hartree) approach, for which up and down spin electrons are independent, and, overestimates configurations with doubly occupied sites. Using the Rayleigh-Ritz principle, this parameter is determined by minimization of the energy in the Gutzwiller state $|\psi_G\rangle$, giving an upper bound to the true but unknown ground state energy of H. To enable a practical calculation, it is necessary to use the Gutzwiller approximation, which assumes that all configurations in the HWF have the same weight.

Nozieres[12] proposed an alternative which shows that the Gutzwiller approach is equivalent to the renormalization of the density matrix in the GWF. It can be formalized as

$$\rho_G = T^{\dagger} \rho_0 T \ . \tag{5}$$

The density matrices $\rho_G = |\psi_G\rangle\langle\psi_G|$ and $\rho_0 = |\psi_0\rangle\langle\psi_0|$ are projectors on the GWF and HWF, respectively. T is an operator which is diagonal in the configuration basis; $T = \Pi_i T_i$ where T_i is a diagonal operator acting on site i:

$$T_i |L_i, L'\rangle = \sqrt{\frac{p(L_i)}{p_0(L_i)}} |L_i, L'\rangle \ . \tag{6}$$

Here, L_i is an atomic configuration of the site i, with probability $p(L_i)$ in the GWF and $p_0(L_i)$ in the HWF respectively, whereas L' is a configuration of the remaining sites of the lattice. Note that this prescription does not change the phase of the wave function as the eigenvalues of the operators T_i are real. The correlations are local, and the configuration probabilities for different sites are independent.

The expectation value of the Hamiltonian is given by,

$$\langle H \rangle_G = \mathrm{Tr}(\rho_G H) \ . \tag{7}$$

The mean value of the on-site operators is exactly calculated with the double occupancy probability, $d_i = \langle n_{i\uparrow} n_{i\downarrow} \rangle_G$. Therefore, the d_i are the new variational parameters replacing g. Using Eqs. (5)-(6), the two-site operator contribution of the kinetic energy can be written as

$$\langle c^\dagger_{i\sigma} c_{j\sigma}\rangle_G = \mathrm{Tr}(\rho_G c^\dagger_{i\sigma} c_{j\sigma}) = \langle c^\dagger_{i\sigma} c_{j\sigma}\rangle_0 \sum_{L_{-\sigma}} \sqrt{\frac{p(L'_\sigma, L_{-\sigma})}{p_0(L'_\sigma)}} \sqrt{\frac{p(L_\sigma, L_{-\sigma})}{p_0(L_\sigma)}} \,, \tag{8}$$

where L'_σ and L_σ are the only two configurations of spin σ at sites i and j that give a non-zero matrix element for the operator in the brackets. The summation is performed over the configurations of opposite spin $L_{-\sigma}$. The probabilities p_0 in the HWF depend only on the number of electrons, whereas the p in the GWF also depends on d_i.

After some elementary algebra, one can show that the Gutzwiller mean value can be factored into

$$\langle c^\dagger_{i\sigma} c_{j\sigma}\rangle_G = \sqrt{q_{i\sigma}} \langle c^\dagger_{i\sigma} c_{j\sigma}\rangle_0 \sqrt{q_{j\sigma}}, \tag{9}$$

where these renormalization factors $q_{i\sigma}$ are local and can be expressed as

$$\sqrt{q_{i\sigma}} = \frac{\sqrt{1 - n_{i\sigma} - n_{i-\sigma} + d_i}\sqrt{n_{i\sigma} - d_i} + \sqrt{d_i}\sqrt{n_{i-\sigma} - d_i}}{\sqrt{n_{i\sigma}(1 - n_{i\sigma})}} \,. \tag{10}$$

In Eq. (9), $\langle c^\dagger_{i\sigma} c_{j\sigma}\rangle_0$ is shorthand for the expectation value of $c^\dagger_{i\sigma} c_{j\sigma}$ over the HWF $|\psi_0\rangle$, and similarly for the average over the Gutzwiller state $|\Psi_G\rangle$. We have also used $n_{i\sigma}$ as shorthand for $\langle n_{i\sigma}\rangle$, that is, the average number of electrons on the considered "orbital-spin" in the HWF. In the simple case when the state is homogeneous and paramagnetic, all quantities becoming site- and spin-independent.

In Eq. (9), the term contributing to the kinetic energy, $\langle c^\dagger_{i\sigma} c_{j\sigma}\rangle_0$, is renormalized by a factor of q, which is less than one in the correlated state, and equal to one in the HWF. This factor can be interpreted as a direct measure of the correlation effect. Indeed Vollhardt[13] has shown that $1/q = m^*/m$ where m^* is the effective mass and m is the bare mass of the electron. Thus a q close to 1 corresponds to a weakly correlated electron system and a smaller q value reflects enhancement of the correlation effect. Equation (7) leads to the variational energy per site, and for the homogeneous and paramagnetic state, is given by

$$E(d) = \langle H\rangle_G = 2q\varepsilon^0_{kin} + Ud \,, \tag{11}$$

which can be minimized numerically with respect to the variational parameter d. In the above expression, the factor 2 accounts for the two-fold spin degeneracy and ε^0_{kin} is the kinetic energy per site and per spin identical at all sites and spins for a homogeneous HWF:

$$\varepsilon^0_{kin} = \sum_j \langle c^\dagger_{i\sigma} c_{j\sigma}\rangle_0 t_{ij} \,. \tag{12}$$

In the case of half filling ($n = 1/2$), minimization is analytical, and provides the optimal choice for double occupancy d:

$$d = \frac{1}{4}\left(1 - \frac{U}{16\varepsilon^0_{kin}}\right) , \tag{13}$$

and

$$q = 1 - \frac{U^2}{(16\varepsilon^0_{kin})^2} \,. \tag{14}$$

If the Coulomb repulsion U exceeds a critical value $U_c = 16\varepsilon^0_{kin}$, $q = 0$, leading to an infinite quasiparticle mass with a Mott-Hubbard Metal-Insulator transition. This is also known as "the Brinkmann-Rice transition",[14] as these authors first applied the Gutzwiller approximation to the Metal-Insulator transition.

Away from half-filling, one has to minimize the variational energy of Eq. (7) numerically. Moreover if the system is spatially inhomogeneous, which is the case for a MD simulation, all quantities (d_i, q_i) may vary locally from one site to the other. Consequently, the general variational energy, a function of double occupancy probabilities d_i on all sites, is

$$E_{var} = \sum_{ij\sigma} \sqrt{q_{i\sigma}} t_{ij} \sqrt{q_{j\sigma}} \langle c^\dagger_{i\sigma} c_{j\sigma}\rangle_0 + \sum_i U d_i \,. \tag{15}$$

Minimization must then be performed numerically for each site, i.e., derivation with respect to d_i, leading to the local equation:

$$\frac{\partial \sqrt{q_{i\sigma}}}{\partial d_i} = \frac{U\sqrt{q_{i\sigma}}}{4|e_{i\sigma}|} \,, \tag{16}$$

for the spin degenerate case. The factor 4 arises from the two-fold spin degeneracy and the Hermiticity. Throughout this work, we limit discussions to the spin degenerate case. We keep the spin index in the relevant physical quantities solely to reminder that these quantities are measured per spin projection. Here $e_{i\sigma}$ is the local partial "effective" kinetic energy, i.e., the contribution of orbital-spin "$i\sigma$" to kinetic energy, calculated with an "effective" hopping:

$$e_{i\sigma} = \sum_j \langle \sqrt{q_{i\sigma}} c^\dagger_{i\sigma} c_{j\sigma}\rangle_0 t_{ij} \sqrt{q_{j\sigma}} \,. \tag{17}$$

This quantity is always negative, which explains the use of its absolute value in Eq. (16).

B. Inequivalent sites: renormalization of levels

When sites are inequivalent, or if orbitals belong to different symmetries as in a multi-orbital basis, it is necessary to add to the Hamiltonian an on-site energy term

$$H_{\text{on-site}} = \sum_{i\sigma} \epsilon^0_{i\sigma} n_{i\sigma} \,. \tag{18}$$

The Hubbard Hamiltonian is then written as

$$H = H_{kin} + \sum_{i\sigma} \epsilon^0_{i\sigma} n_{i\sigma} + U \sum_i n_{i\uparrow} n_{i\downarrow} \ , \qquad (19)$$

with H_{kin} given by Eq. (2). In this case, the starting HWF directly obtained from the non-interacting part of the Hamiltonian, is not automatically the optimal choice, i.e., having the lowest energy. When we look for the ground state of Eq. (19) in the Hartree-Fock (HF) self-consistent field formalism, it is necessary to vary the orbital occupations. Practically, it can be achieved by replacing Eq. (19) by an effective Hamiltonian $H_{\rm eff}$ of independent particles with renormalized on-site energies $\epsilon_{i\sigma}$:

$$H_{\rm eff} = \sum_{i\neq j,\sigma} t_{ij} c^\dagger_{i\sigma} c_{j\sigma} + \sum_{i\sigma} \epsilon_{i\sigma} n_{i\sigma} + C \ . \qquad (20)$$

The HWF we seek is an *approximate* ground state of the *true* many-body Hamiltonian (19) and is the *exact* ground state of *effective* Hamiltonian (20). The additive constant C accounts for the double counting energy, so that the ground state energies are the same for both Hamiltonians:

$$\langle H_{\rm eff} \rangle = \langle H \rangle \ . \qquad (21)$$

The optimal choice of parameters $\epsilon_{i\sigma}$ can be obtained by minimizing the ground state energy of $H_{\rm eff}$ with respect to $\epsilon_{i\sigma}$. Invoking the Hellmann-Feyman theorem, one can obtain the derivative of the kinetic energy

$$\frac{\partial \langle H_{kin} \rangle}{\partial \epsilon_{i\sigma}} = - \sum_{j\neq i,\sigma} \epsilon_{j\sigma} \frac{\partial \langle n_{j\sigma} \rangle}{\partial \epsilon_{i\sigma}} \ . \qquad (22)$$

By taking a mean-field approximation $\langle n_{i\uparrow} n_{i\downarrow} \rangle \approx \langle n_{i\uparrow} \rangle \langle n_{i\downarrow} \rangle$, and performing a partial derivative on both sides of Eq. (21) with respect to $\epsilon_{l\sigma'}$, and comparing the coefficients before the factor $\frac{\partial \langle n_{i\sigma} \rangle}{\partial \epsilon_{l\sigma'}}$, we recover the well-known formula for the on-site energies:

$$\epsilon_{i\sigma} = \epsilon^0_{i\sigma} + U \langle n_{i-\sigma} \rangle \ , \qquad (23)$$

which is usually obtained from a direct mean-field decoupling. Here the constant C is simply $-U \sum_i \langle n_{i\uparrow} \rangle \langle n_{i\downarrow} \rangle$.

In the Gutzwiller approach, the same argument about the variation of orbital occupation, i.e., flexibility on the HWF $|\psi_0\rangle$, is true. It is necessary to find a way to vary this Slater determinant, from which the GWF $|\Psi_G\rangle$ is generated, so that the Gutzwiller ground-state energy is a minimum. One needs to find an equivalent of Eq. (23) in the Gutzwiller context. The average value of Eq. (19) is given by:

$$\langle \Psi_G | H | \Psi_G \rangle = \sum_{ij\sigma} t_{ij} \sqrt{q_{i\sigma}} \langle c^\dagger_{i\sigma} c_{j\sigma} \rangle_0 \sqrt{q_{j\sigma}} + U \sum_i d_i + \sum_{i\alpha\sigma} \epsilon^0_{i\sigma} \langle n_{i\sigma} \rangle_0 \ . \qquad (24)$$

Following the previous HWF self-consistent field approach, one can find an effective Hamiltonian $H_{\rm eff}$ of independent particles having $|\psi_0\rangle$ as an *exact* ground state. This state $|\psi_0\rangle$ generates the GWF $|\Psi_G\rangle$ which is an *approximate* ground state of the true Hamiltonian Eq. (19). In analogy with Eq. (21),

$$\langle \psi_0 | H_{\rm eff} | \psi_0 \rangle = \langle \Psi_G | H | \Psi_G \rangle \ , \qquad (25)$$

leads to the expression:

$$H_{\rm eff} = \sum_{i\neq j,\sigma} \tilde{t}_{ij} c^\dagger_{i\sigma} c_{j\sigma} + \sum_{i\sigma} \epsilon_{i\sigma} n_{i\sigma} + C' \ , \qquad (26)$$

with effective but *fixed* renormalized hopping integrals $\tilde{t}_{ij} = \sqrt{q_{i\sigma}} t_{ij} \sqrt{q_{j\sigma}}$ and effective on-site energies $\epsilon_{i\sigma}$, still to be determined. The Hellmann-Feynman theorem applied to $H_{\rm eff}$ provides again an expression similar to Eq. (22), but with effective hopping integrals. Taking into account the dependence of the $q_{i\sigma}$'s through $n_{i\sigma}$ (Eq. (10)) and differentiating Eqs. (24) and (25) with respect to the parameters $\epsilon_{i\sigma}$, one obtains the equivalent expression to Eq. (23) in the Gutzwiller context:

$$\epsilon_{i\sigma} = \epsilon^0_{i\sigma} + 2 e_{i\sigma} \frac{\partial \ln(\sqrt{q_{i\sigma}})}{\partial n_{i\sigma}} \ . \qquad (27)$$

Here $e_{i\sigma}$ is the partial kinetic energy of orbital-spin $i\sigma$:

$$e_{i\sigma} = \sum_{j\sigma} \tilde{t}_{ij} \langle c^\dagger_{i\sigma} c_{j\sigma} \rangle_0 = \int_{-\infty}^{\rm E_F} E \tilde{N}_{i\sigma}(E) dE - \epsilon_{i\sigma} \langle n_{i\sigma} \rangle_0 \ , \qquad (28)$$

with $\tilde{N}_{i\sigma}$ the $i\sigma$-projected density of states (DOS) for a system described $H_{\rm eff}$. Equation (25) leads to

$$C' = U \sum_i d_i - \sum_{i\sigma} 2 e_{i\sigma} \frac{\partial \ln(\sqrt{q_{i\sigma}})}{\partial n_{i\sigma}} \langle n_{i\sigma} \rangle \ . \qquad (29)$$

Except for a few very special conditions in one-band Hubbard model, the renormalization of correlated-orbital levels is not only important in the optimization of the total energy but also in giving a correct description of single-particle quasiparticle properties.[15] To solve the full problem of finding an approximate ground state to Eq. (19), one is faced with a self-consistency loop: First get the occupations $\langle n_{i\sigma} \rangle_0$ from a HWF, and a set of 'bare' $\epsilon^0_{i\sigma}$ levels; then obtain a set of configuration parameters, the probabilities of double occupation, d_i by minimizing Eq. (24) with respect to these probabilities, followed by the on-site level renormalization according to Eq. (27). The loop is repeated until a convergence is achieved.

III. APPROXIMATIONS FOR FAST CORRELATED ELECTRONIC STRUCTURE

A. Approximated solutions of Gutzwiller minimization

Due to the complicated expression of Eq. (10), it is non-trivial to solve Eq. (16). Graphically, the solution

corresponds to the intersection of the function $\frac{\partial\sqrt{q_{i\sigma}}}{\partial d_i}$ with a horizontal line $U/4|e_{i\sigma}|$ (see Fig. 1).

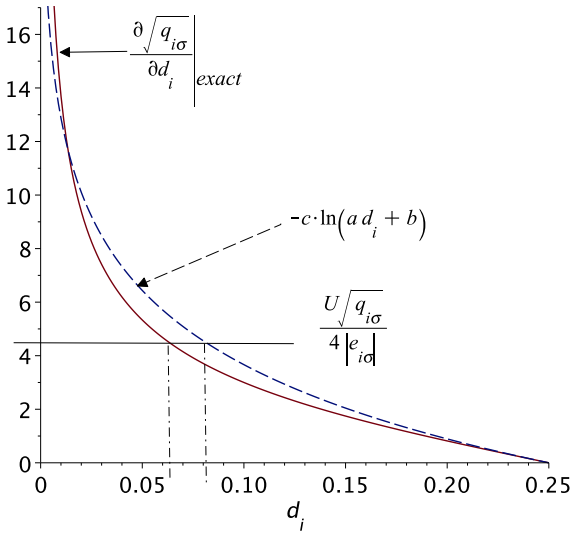

FIG. 1. (Color online) The exact (full line) and approximate (dashed line) $\partial\sqrt{q_{i\sigma}}/\partial d_i$ as a function of d_i.

This situation will affect applications of the Gutzwiller method to MD, as analytical expressions are desirable to derive forces on the atoms. Fortunately, the function $\frac{\partial\sqrt{q_{i\sigma}}}{\partial d_i}$ can be fitted with reasonable accuracy (see Fig. 1) by a logarithm function, giving an analytical approximate solution d_i of Eq. (16). This choice was suggested by the shape of the true derivative of $\sqrt{q_{i\sigma}}$, with the following physical constraints: The uncorrelated case ($U = 0$) has to give the solution $d_i = n_{i\sigma}^2$, for a given occupancy $n_{i\sigma}$, and the probability of double occupancy d_i is restricted in the range $\max(0, 2n_{i\sigma} - 1) < d_i < n_{i\sigma}$ (otherwise there would be negative arguments in the square root of q), providing a rescaling of the logarithm argument. Finally, we determine the coefficient in front of the logarithm, such that the fitted function has the same slope as the true one in the uncorrelated limit $n_{i\sigma}^2$. The final result reads:

$$\frac{\partial\sqrt{q_{i\sigma}}}{\partial d_i} \simeq -c\ln(ad_i + b) \tag{30}$$

The physical constraints above fix uniquely all three coefficients

$$a = \frac{1}{n_{i\sigma}^2 - \max(0, 2n_{i\sigma} - 1)}\ , \tag{31}$$

$$b = -a\,\max(0, 2n_{i\sigma} - 1)\ , \tag{32}$$

$$c = \frac{n_{i\sigma}^2 - \max(0, 2n_{i\sigma} - 1)}{4n_{i\sigma}^3(1 - n_{i\sigma})^3}\ . \tag{33}$$

Within this approximation, the approximate value of double occupancy, as the solution of the minimization equation, is $d_i = (n_{i\sigma}^2 - d_i^m)\exp(-U/4|e_{i\sigma}|) - d_i^m$, where $d_i^m = \max(0, 2n_{i\sigma} - 1)$. The small remaining difference between this approximate and the true value can be corrected by a second order expansion around the approximate value d_i leading to a more accurate analytical expression

$$d_i^{2nd} = d_i - \frac{f' + \sqrt{f'^2 - 2f''[f + c\ln(ad_i + b)]}}{f''}\ . \tag{34}$$

Here f, f', and f'' stand for the true $\frac{\partial\sqrt{q_{i\sigma}}}{\partial d_i}$, and its first and second order derivatives, respectively, calculated at the approximated value d_i.

The relative error of this second order corrected value with respect to the exact solution is less than 1% over the whole range of values. Thus, this second order corrected local double occupancy is used in the calculation of renormalization factor $\sqrt{q_{i\sigma}}$, Eq. (10). To check the validity of this approximation for the derivative, we also plot in Fig. 1 the comparison between true and approximate $\sqrt{q_{i\sigma}}$. Again we see the good accuracy, with a small discrepancy occuring in the range of very small double occupancy, i.e., corresponding to high values of Coulomb repulsion U, not often encountered for realistic materials.

B. Second moment approximation (SMA): An efficient tool for kinetic energy evaluation

The other input for Eq. (28) necessary to perform tractable MD simulations is the partial kinetic energy. A common approximation is the well-known approach of second moments.[16] It is supported by the observation that all necessary quantities for the energetics are integrated quantities. Consequently, they are not too sensitive to the fine details of the DOS, which can be approximated by a rectangular electronic density of states of bandwidth $W_{i\sigma}$ and height $1/W_{i\sigma}$ for each orbital and spin. The second moment of the rectangular DOS, equal to $\epsilon_i^2 + \frac{W_i^2}{12}$, is set equal to the real one obtained from closed loop paths counting $\langle i|H^2|i\rangle = \epsilon_i^2 + \sum_j t_{ij}^2$, determining the bandwidth $W_{i\sigma}$.

Practically, for a given MD snapshot, the second moment for a given atomic site "i" can be constructed as a sum over atoms "j" neighboring "i" as $\mu_{2,i} = \sum_j t_{ij}^2$ (see Appendix for more details). Using the simple tight-binding theory,[17] the hopping integrals t_{ij} scale as a power law of the interatomic distance $r_{ij} = |\mathbf{r}_i - \mathbf{r}_j|$. With the number of electrons on each atom (assuming charge neutrality for all sites), the partial kinetic energy, needed as input in Eq. (28), is given by $e_{i\sigma} = W_{i\sigma}n_{i\sigma}(n_{i\sigma} - 1)/2$, similar to the result by Ackland.[18] To compute μ_2 and to account for the effect of Coulomb correlations, we use the hopping integrals renormalized by q-factors, $\sqrt{q_i}t_{ij}\sqrt{q_j}$, rather than the bare ones, t_{ij}: After minimization in the Gutzwiller method, the true interacting Hamiltonian H is replaced by an effective Hamiltonian of non-interacting quasiparticles similar to (26), with renormalized hopping integrals. Potentially the on-site energies need to be renormalized too, but it is not necessary in our case, as we

assumed charge neutrality, so there is no average charge transfer between sites. To conclude, we show that inclusion of electronic correlations in MD simulations within the Gutzwiller method just requires one more intermediate step, compared to usual one, with renormalization factors that reduce the values of the hopping integrals. Once computed for a set of actual positions of atoms, the rest of the process is similar to other semi-empirical approaches.[8,19]

IV. FORCES FOR MD

For a given set of atomic positions, the overall total energy of the system is the sum of the electronic approximate Gutzwiller ground state energy E_G plus a short range repulsion potential,

$$E_{tot} = E_G + E_{\rm rep} \ . \tag{35}$$

The x-component of the force acting on atom i, $F_{x,i}$ is the derivative of E_{tot} with respect to position component x_i of this atom (same relations hold for y- and z-components):

$$\begin{aligned} F_{x,i} &= -\frac{dE_{tot}}{dx_i} \\ &= -\sum_j \left(\frac{\partial E_G}{\partial d_j}\frac{\partial d_j}{\partial x_i} + \frac{\partial E_G}{\partial n_{jf}}\frac{\partial n_{jf}}{\partial x_i}\right) - \frac{\partial E_G}{\partial x_i} - \frac{\partial E_{\rm rep}}{\partial x_i} \\ &= -\frac{\partial E_G}{\partial x_i} - \frac{\partial E_{\rm rep}}{\partial x_i} \ , \end{aligned} \tag{36}$$

since the first two terms in the second line are zero because of Gutzwiller optimizations with respect to double, d_j and single, n_{jf} occupancies respectively. From the Hellmann-Feynman theorem, the first term, due to the hybridization, can be split into elementary contributions:

$$\frac{\partial E_G}{\partial x_i} = \sum_{j\neq i}\sum_{\alpha\beta} f^{(x)}_{i\alpha j\beta} \ , \tag{37}$$

where the contribution of orbitals α of site i and β of site j (α or β are either d- or f-orbitals) is related to the derivative of the hopping integral $t_{i\alpha j\beta}$,

$$f^{(x)}_{i\alpha,j\beta} = -\frac{\partial t_{i\alpha,j\beta}}{\partial x_i} 4\sqrt{q_i}\langle c^\dagger_{i\alpha\sigma} c_{j\beta\sigma}\rangle \sqrt{q_j} \ . \tag{38}$$

For the interacting case ($U \neq 0$), $\sqrt{q_i}$ or $\sqrt{q_j}$ are less than one for correlated-orbitals but equal to one for non-correlated-orbitals. For the non-interacting case ($U = 0$), the above formula is obtained by setting all $q = 1$. It can be shown that forces due to hybridization are always attractive.

Formula (38) requires knowledge of the mean value of the hopping operator. If the eigenstates are known, as in the case of the exact diagonalization, one can exactly calculate this value (see Appendix). If using SMA, it is possible to calculate an approximate value of this average by generalizing this approximation to off-diagonal elements of Green function. However, contrary to the exact diagonalization, we cannot apply the Hellmann-Feynman theorem and the result is a small difference of location between the energy minimum and the zero of forces. We overcome this problem by replacing the exact Hamiltonian by a Hamiltonian approach based on SMA, in which the terms of partial local kinetic energies are replaced by their approximations, $e_{i\alpha} = \frac{1}{2} W_{i,\alpha} n_{i\alpha}(n_{i\alpha} - 1)$ and the bandwidth of the density of states projected onto the orbital $|i\alpha\rangle$, $W_{i\alpha} = \sqrt{12 \sum_{j\beta} \tilde{t}^2_{i\alpha,j\beta}}$. In this approach, partial occupancies at zero temperature are simply given by $n_{i\alpha} = \frac{1}{2} + \frac{E_F - \epsilon_{i\alpha}}{W_{i\alpha}}$, where E_F is the Fermi level of the system. Here, in the case of correlated systems, the hopping integrals $\tilde{t}_{i\alpha,j\beta}$ are connected to the real $t_{i\alpha,j\beta}$ by the Gutzwiller renormalization factors $\sqrt{q_{i\alpha}}$, $\sqrt{q_{j\beta}}$. By applying this to the effective Hamiltonian (26) and replacing spin index σ by a more general orbital-spin index α, we can write the approximated SMA Hamiltonian as

$$H_{\rm SMA} = \sum_{j,\alpha} \frac{1}{2} W_{j,\alpha} n_{j\alpha}(n_{j\alpha} - 1) + \epsilon_{j\alpha} n_{j\alpha} + C' \ . \tag{39}$$

The advantage of this approach is that, by construction, the minimum energy location coincides exactly with the location of zero forces by allowing the application of the Hellmann-Feynman theorem. Finally, note that this approach based on an energy expressed in the SMA is similar to Ackland and Reed.[18] With the above formulas one can establish that the force experienced by the atom i is expressed as

$$F_{x,i} = -\sum_{j,\alpha} \frac{\partial W_{j,\alpha}}{\partial x_i} \frac{1}{2} n_{j\alpha}(n_{j\alpha} - 1) - \frac{\partial E_{\rm rep}}{\partial x_i} \ . \tag{40}$$

The dependence of $W_{j,\alpha}$ on hopping integrals $t_{i\alpha,j\beta}(|\mathbf{r}_i - \mathbf{r}_j|)$, enables an explicit expression for the force, depending on the model under consideration as discussed in next section. The computed forces Eq. (36) for ED or Eq. (40) for SMA, are then inserted into Newton's equation of motion (EOM) for each atom. The positions are advanced in time by a time step δt by numerically integrating the EOMs with the Verlet algorithm. The resulting new atomic positions are then taken as input into Eq. (26), and new atomic forces Eq. (36) or Eq. (40) are computed. The MD trajectory consists of the string of many time steps iterating back and forth through this two-step process.

V. MODEL AND RESULTS

A. Model

To illustrate the method, we consider a minimal two-orbital model that mimics, e.g., heavy fermions or actinides systems, with one non-correlated band, called for convenience "d", whereas the other, called "f", possesses

a strong local Coulomb repulsion U. For simplicity, each of these two orbitals has a spin-$\frac{1}{2}$ degree of freedom. This model is described by the following Hamiltonian (close in spirit to the Anderson lattice model) with the usual notation:

$$H = \sum_{i\neq j,\sigma}\left[t_{id,jd}c^{\dagger}_{id\sigma}c_{jd\sigma} + t_{id,jf}c^{\dagger}_{id\sigma}c_{jf\sigma} + t_{if,jd}c^{\dagger}_{if\sigma}c_{jd\sigma}\right] + \sum_{i\sigma}(\epsilon^{0}_{id\sigma}n^{d}_{i\sigma} + \epsilon^{0}_{if\sigma}n^{f}_{i\sigma}) + \sum_{i} U n^{f}_{i\uparrow}n^{f}_{i\downarrow}\ . \quad (41)$$

Here the d-orbitals are coupled among themselves and with f-orbitals, whereas the f-orbitals are only coupled to their neighboring d-orbitals. The power laws[17] in distance from atom located at position r_i to atom at r_j for hopping integrals dd-coupling and df-coupling are respectively:

$$t_{id,jd} = t_{dd,0}\frac{r_0^5}{|r_i - r_j|^5}\ , \quad (42)$$

and

$$t_{id,jf} = t_{df,0}\frac{r_0^6}{|r_i - r_j|^6}\ , \quad (43)$$

where $t_{dd,0}$ and $t_{df,0}$ are constants, r_0 is a reference unit of length used in our calculations. After the Gutzwiller variational treatment of Hamiltonian Eq. (41), we obtain

$$H_{\rm eff} = \sum_{i,j,\sigma} t_{id,jd}c^{\dagger}_{id\sigma}c_{jd\sigma} + \sum_{i,j,\sigma}[t_{id,jf}\sqrt{q_j}c^{\dagger}_{id\sigma}c_{jf\sigma} + \text{H.c.}] + \sum_{i\sigma}(\epsilon_{id\sigma}n^{d}_{i\sigma} + \epsilon_{if\sigma}n^{f}_{i\sigma}) + \sum_{i} U_i d_i + C'\ , \quad (44)$$

whose parameters are obtained from the minimization procedure analogous to deriving Eq. (26) from Eq. (25), for a given set of atomic positions. When the converged Gutzwiller ground state for the electronic degrees of freedom has been obtained, we calculate the forces on each atom. These attractive forces have a quantum origin, due to the hybridization through the hopping integrals. Finally, a phenomenological repulsive potential between atoms is added:

$$E_{\rm rep} = \frac{1}{2}\sum_{ij}\frac{\Lambda_0 r_0^{12}}{|\mathbf{r}_i - \mathbf{r}_j|^{12}}\ , \quad (45)$$

with Λ_0 a constant.

Within this particular model, application of formula (40) gives the following explicit expression of the x-component of the force acting on atom i:

$$F_{x,i} = 12\sum_{j\neq i}\Bigg\{\frac{n_{jd}(n_{jd}-1)}{W_{jd}}(5t^2_{jdid} + 6q_{if}t^2_{jdif}) + \frac{n_{id}(n_{id}-1)}{W_{id}}(5t^2_{idjd} + 6q_{jf}t^2_{idjf}) + \frac{n_{jf}(n_{jf}-1)}{W_{jf}}(6q_{jf}t^2_{jfid}) + \frac{n_{if}(n_{if}-1)}{W_{if}}(6q_{if}t^2_{ifjd}) + \frac{\Lambda_0}{|\mathbf{r}_i - \mathbf{r}_j|^{12}}\Bigg\}\frac{x_i - x_j}{|\mathbf{r}_i - \mathbf{r}_j|^2}\ , \quad (46)$$

and a similar expression holds for the y-component. Here the f-orbital bandwidth W_{if} (or W_{jf}) is the bare one renormalized by Gutzwiller factor, i.e. $W_{if} = W^0_{if}\sqrt{q_{if}}$.

As a demonstration, we studied different geometries and number of atoms both with SMA and ED: dimer, trimer, and 1600 atoms in two dimension. For the latter case, we used both open boundary conditions, i.e., a cluster of 1600 atoms isolated in space, and periodic boundary conditions, within the minimum image convention (MIC)[23] to avoid boundary effects. In all calculations, we take $t^0_{dd} = -1t$, $t^0_{df} = 0.5t$, and $\Lambda_0 = 0.4t$. Hereafter all energies are measured in units of t. The bare f level is chosen to be $\epsilon^0_{if\sigma} = -U/2$. To illustrate a realistic order of magnitude, we fix $t = 0.5$ eV and the length unit $r_0 = 4$ Å.

B. Simple analytical cases: dimer and trimer

The dimer and trimer have simple geometries, where all calculations, both ED and SMA, can be performed analytically. This way, we can easily compare both methods and have an estimate of the systematic error made with the approximation in the uncorrelated case ($U = 0$). Ground state energies and equilibrium distances are summarized in Table I. Kinetic energies are also displayed for comparaison with values given in Tables II and III.

The case of the dimer is presented here to illustrate the approach. The exact solution arises from the diagonalization of the Hamiltonian matrix for a given spin polarization

$$\begin{pmatrix} \epsilon_d & 0 & t_{dd} & t_{df} \\ 0 & \epsilon_f & t_{fd} & 0 \\ t_{dd} & t_{df} & \epsilon_d & 0 \\ t_{fd} & 0 & 0 & \epsilon_f \end{pmatrix}$$

Then, in an independent electron picture, one fills the lowest energy states with four electrons for a half-filled system. The total energy of the system is the sum of electronic energy and repulsion terms. With the chosen values of on-site energies and taking into account the spin degeneracy, one obtains

$$E^{\rm ED}_{\rm tot} = -2\sqrt{t^2_{dd} + 4t^2_{df}} + \frac{\Lambda_0}{r^{12}}\ . \quad (47)$$

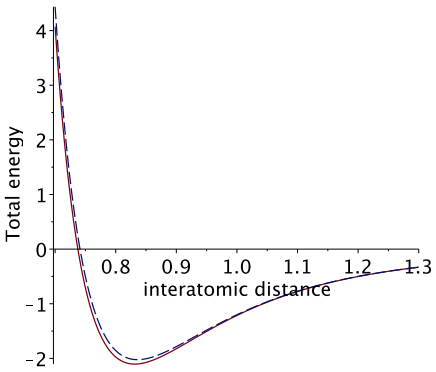

FIG. 2. (Color online) Total energy (in eV) versus interatomic distance (in units of r_0) for the dimer calculated with exact diagonalization (solid line) and with the second moment approximation (dashed line) in uncorrelated case ($U = 0$).

Using the hopping integrals given by Eqs. (42) and (43), one calculates the force experienced by an atom according to Eqs. (37) and (38). The equilibrium interatomic distance is obtained when this force cancels out.

The treatment of the same problem by the SMA method provides the approximated total energy for the half-filled case:

$$E_{\rm tot}^{\rm SMA} = -\sqrt{3}(\sqrt{t_{dd}^2 + t_{df}^2} + \sqrt{t_{df}^2}) + \frac{\Lambda_0}{r^{12}} \,. \qquad (48)$$

From this expression, the same approach as in the ED case yields the force experienced by an atom through Eq. (40), or (46) applied for this diatomic case, and to obtain the equilibrium interatomic distance. The comparison between the ED and SMA total energies as a function of the interatomic distance is shown in Fig. 2. It is to be seen the very good agreement between the exact solution and the approximation. We should note that the good agreement of the ED dimer with its SMA counterpart might be coincidental since replacing the exact DOS with only 4 delta-functions by a rectangular DOS is an extreme limit of the approach.

The same analytical approach may still be made in the case of the trimer, yielding a 6×6 matrix to diagonalize. Again we found a very good agreement of results between the SMA and the ED, as shown in Table I.

Within the Gutzwiller method, we have calculated the equilibrium distance of the dimer as a function of the interaction U (Fig. 3) in the SMA. We have also computed, for $U = 4t$, the total energy as a function of the interatomic distance (Fig. 4(a)) and the force as a function of the interatomic distance too (Fig. 4(b)). Notably, the distance corresponding to minimum of energy precisely coincides with that of the zero force. We also used these analytical calculations to benchmark our codes for arbitrary number of atoms as explained in the next subsection.

	ED (eV/at)	SMA (eV/at)	deviation (%)
Dimer			
E_g	-1.052	-1.013	3.7
E_{kin}	-1.970	-1.872	5.0
interatomic distance	0.8313	0.8358	0.5
Trimer			
E_g	-0.987	-1.067	8.1
E_{kin}	-1.838	-1.967	7.0
interatomic distance	0.8863	0.8821	0.4

TABLE I. Comparaison of ground state energy E_g, kinetic energy E_{kin} and equilibrium interatomic distance between exact diagonalization (ED) and second moment approximation (SMA) for dimer and trimer in the uncorrelated case ($U = 0$).

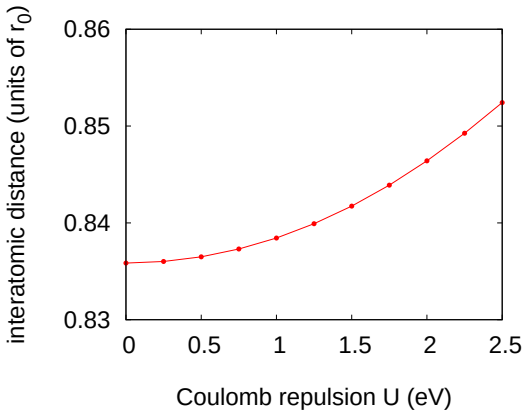

FIG. 3. (Color online) Equilibrium interatomic distance versus U for the dimer calculated with the Gutzwiller method in the SMA.

C. Cluster of atoms

To benchmark our method and illustrate the efficiency of the SMA with approximate solution for double occupancy, we also performed the calculation based on exact diagonalization. Since we are interested in finding only the equilibrium structure of the system, the velocity on each atom is set to zero before advancing by Δt the numerical solution of the EOM. The time step Δt in our practical units was set to 10^{-2} corresponding to a real time of 8.8 femtosecond with a mass of Pu atom, which is in the reasonible order of magnitude of usual MD simulation[22]. The resulting MD "trajectory" eventually finds a local minimum on the energy landscape as the atomic positions are converged and the residual forces are driven to the noise limit.

We started with an initial condition of a regular square lattice of 40×40 atoms in a two dimensional cluster with open boundary conditions. After 100,000 MD iterations, we obtained the two snapshots of atomic positions as shown in Fig. 5 from the ED and SMA methods, respectively. An important advantage of the SMA calculation is a calculation two orders of magnitude faster

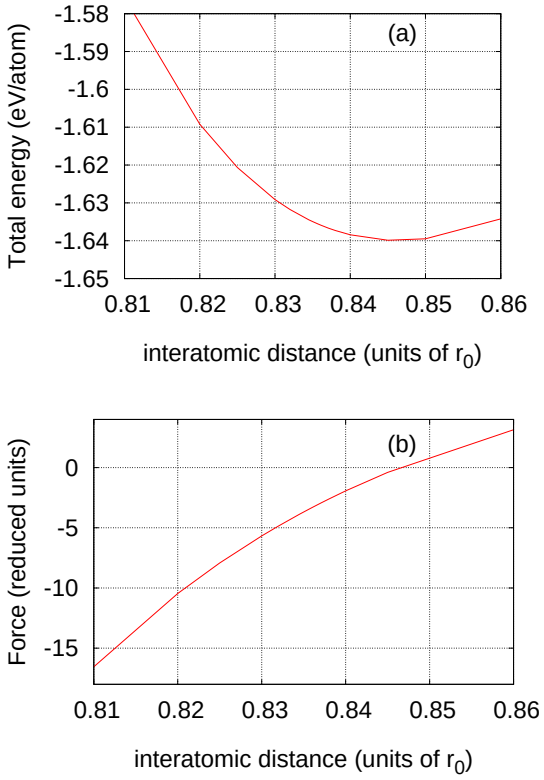

FIG. 4. (Color online) Total energy (a) and force (b) versus interatomic distance for the dimer calculated with the Gutzwiller method in the SMA for $U = 4t$.

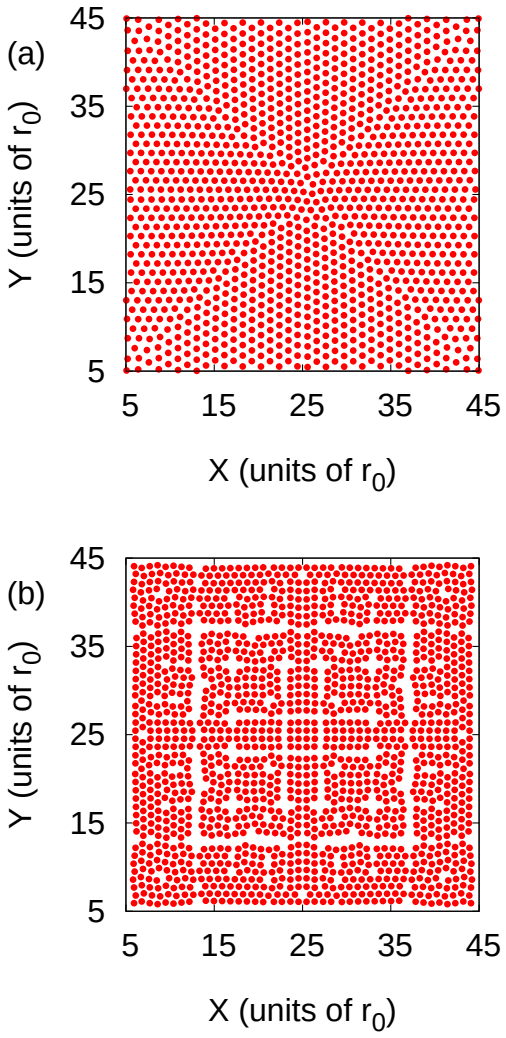

FIG. 5. (Color online) Snapshot of atomic positions obtained from exact diagonalization (a) and the SMA (b) for a cluster of 1600 atoms, with open boundary conditions, after 100,000 MD steps from ordered initial conditions (see text).

than ED. These snapshots, even if they are far from being converged (total energy has not yet reached a constant limit), tend to form a hexagonal local order. Moreover, both patterns also keep the same overall symmetries of their initial square lattice-like structure with obvious four mirror-symmetry axes, each of them being shifted from its two neighboring axes by 45°. Starting with the same initially ordered structure, the system is trapped into metastable states, which have the same symmetries as the initial one. This artificial effect does not happen when we performed a true MD calculation, as discussed later in Section D, where the velocity of atoms adds randomness to smear out the memory of initial conditions.

To avoid edge effects (surface effects in a three-dimensional case), we considered a periodic replication of the initial cluster in both ordered and randomized structures. Starting from these two different initial conditions, we performed MD simulations with the ED and SMA codes, both using the minimum image convention (MIC).[23] The effect of this approximation will be discussed later. After MD steps and minimization on the overall total energy by tuning the size (x and y-directions) of the periodic box containing the initial cluster, iterations in both ED and SMA approaches converged to a unique hexagonal close-packed structure. The only difference between ED and SMA is a slightly different equilibrium interatomic distance ($d_0^{\rm ED} = 0.9852 r_0$ versus $d_0^{\rm SMA} = 0.9605 r_0$).

Now, to evaluate the influence of the different approximations made above, we studied the SMA results against the ED ones, both in the MIC and in the conventional analytical momentum-space solution since the converged structure is a regular hexagonal lattice. To this aim, we performed one single iteration in the hexagonal structure at the interatomic distance that minimizes the SMA total energy, to compute the kinetic energy with the SMA and ED within MIC, and ED in the momentum-space.

Exact diagonalization with MIC. In the MIC, electrons on an atom close to the boundary of a supercell are allowed to interact (via the hopping) with those on the image atoms belonging to the closest neighboring supercell. It essentially establishes the interactions between

	ED	**SMA**	Deviation (%)
Numerical (MIC)	-1.7984	-2.1419	16.0
Analytical (**k**-space)	-1.8012	-2.1413	15.9
Deviation (%)	0.155	0.028	

TABLE II. Comparison of kinetic energy (in units of eV/atom) between ED within the MIC or within **k**-space and SMA for one MD iteration for the uncorrelated case ($U = 0$).

electrons on the boundary of the original supercell with those on the opposite sides of the supercell, which are usually quite far away. The use of MIC is equivalent to performing Γ-point-only (i.e., $\mathbf{k} = 0$ in the first Brillouin zone) calculations in the reciprocal space from the Bloch theorem, for which the Hamiltonian for the supercell is modified by the phase factor $\exp(i\mathbf{k} \cdot \mathbf{R})$ with $\mathbf{R}$ the lattice vectors. Naturally, the MIC treatment will be more suitable for larger systems. Since SMA is based on the surrounding of an atom, it is much less sensitive to the system size within MIC.

Exact diagonalization in the reciprocal space of the minimal unit cell. Since the converged hexagonal structure has a translational symmetry with a unit cell containing one atom, we can perform an exact diagonalization calculation in the reciprocal space of 2×2 Hamiltonian matrices. In the calculations, we have kept the hopping integrals up to 3-rd nearest-neighbors. A regular mesh of **k**-mesh was generated in the first Brillouin zone. The eigenvalues are then summed up to the Fermi level over all **k**-points for the band-energy. The grid of the **k**-mesh is determined with the band-energy varying no larger than 10^{-5}%.

A summary of the results for 1600 atoms is presented in Table II. Here only a single iteration was made for the same structure (hexagonal) with the same interatomic distance to compare kinetic energy with both methods. In Table II, we also list the converged results calculated analytically from the momentum space with the hopping integrals kept up to 3-rd nearest-neighbors (for both ED and SMA methods). We note that since the short range repulsion (i.e., the term in r^{-12}) is exactly the same (same structure, same distance) for all cases, only kinetic energies are given in this table. With each approach, the agreement of results between numerical and analytical calculations are excellent (deviation 0.155 % for ED while 0.028 % for SMA). We see that the influence of MIC in the ED code with respect to exact calculation (k-space no MIC) is reduced relatively (0.155% relative deviation) and also we see that the SMA is much less sensitive to MIC (even better agreement between analytical and numerical results: 0.028%) The difference of the energy between SMA and ED numerical calculations in real space is inherent to the SMA approximation itself since almost the same deviation is also observed in analytical calculations in momentum space.

Furthermore, our analytical results show that, although the kinetic energy obtained from both methods differs by 16% (see Table II), the equilibrium interatomic distance deviates only by 2.5 percent. It suggests the SMA is a reliable method to predict the structure of systems.

	MIC	**k**-space	Deviation (%)
SMA			
16 atoms	-2.1409	-2.1413	0.017
1600 atoms	-2.1419	-2.1413	0.028
ED			
16 atoms	-1.7207	-1.8012	4.5
1600 atoms	-1.7984	-1.8012	0.155

TABLE III. Comparison of energy (in units of eV/atom) for clusters of 16 and 1600 atoms calculated in the SMA (MIC) and ED (MIC) methods with that analytically calculated in the **k**-space calculation for one single-shot MD iteration in the uncorrelated case ($U = 0$).

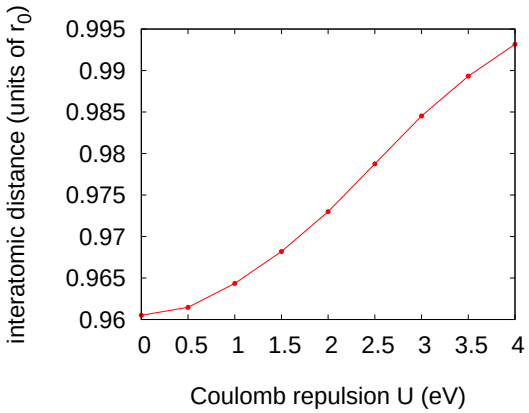

FIG. 6. (Color online) Dependence of the interatomic equilibrium distance on U from the GA-MD simulations with the SMA on a 40×40-atom cluster with MIC.

Size effect in the real-space calculations. We have performed calculations on a smaller cluster with 4×4=16 atoms from both SMA and ED with MIC periodic boundary conditions, and compare the results with the analytical solutions of an infinite hexagonal structure. The kinetic energies are shown in Table III. It is seen that the deviation in the SMA method even for such a small system is small and is comparable to that for the system with 1600 atoms. However, with the ED method, the deviation for the 16-atom system is much larger than that for the 1600-atom one.

Finally, we applied the full Gutzwiller plus MD within the SMA to the 1600 atoms cluster with MIC for various values of repulsion U ranging from 0 to $8t$. The U-dependence of the equilibrium interatomic distance is shown in Fig. 6. As expected and in accordance to our previous experiences with δ-Pu,[5] we see that the Gutzwiller q-factors have the effect of reducing the hybridization and the resultant attractive forces, which

leads to a slightly more expanded equilibrium structure. The same trend was also observed in the results (not shown here) obtained by exact diagonalization with $U = 0$ versus $U = 4t$, and also for the dimer case presented above. We note that the structure expansion is small, around 4% of the interatomic distance for the uncorrelated case. The reason lies in the fact that in the Anderson-like model, the attractive force arises not only from the d-f hybridization hopping but also significantly from the direct d-d hopping. In addition, the efficiency of the hybridization reduction in the present model is proportional to $\sqrt{q_i}$. It is in contrast to the one-orbital Hubbard model, where the effective hopping integrals are proportional to $\sqrt{q_i}\sqrt{q}_j$.

D. Temperature effects and MD

We have also relaxed the infinite damping limit for the velocities we used in preceding sections and perform true MD simulations. The temperature was fixed with the gaussian thermostat.[23] The simulations were carried out for 64 atoms in periodic boundary conditions with a box length equal to the equilibrium value at $T = 0$ for a given value of U (see Fig. 4). We have studied the effect of electronic correlation on the radial distribution function $g(r)$. In the first set of calculations, we fixed the Coulomb interaction parameter U to 2 eV and considered the evolution of $g(r)$ as a function of temperature ranging from 300 K to 6000 K (see Fig. 7). The positions of the peaks at the lowest temperature are centered at the positions of the $T = 0$ ground state structure (not shown in the figure). We observe two features: the position of the first peak moves slowly towards smaller distances while the temperature is increased. At the same time, the intensity of the peaks decreases and the dips fill in. Noticeably, at the highest temperatures (3000 K and 6000 K), the dip fills in for $g(r) \sim 0.5$; this is suggestive of the beginning of melt transition, which is in the range of the melting temperature for all known metals. It can also be seen that the second and third peak coalesce at $T = 1500$ K whereas the same trend occurs for the fourth and the fifth peak.

In the second set of calculations, we considered the evolution of $g(r)$ for a given temperature $T = 300$ K, versus the Coulomb interaction U ranging from 0 to 4 eV. Figure 8 showst $g(r/r_0)$ for different values of U, where r_0 is the $T = 0$ equilibrium value for a given value of U. (Since the curve with $U = 3$ eV is almost superimposed on that with $U = 4$ eV, we do not show it in the figure). For a given peak, the center of the peak in scaled distance r/r_0, and thus the structure, is the same as a function of U. The first peak is almost the same height for all values of U. For the subsequent peaks, each of the peaks broaden (heights decrease and the dips increase) due to the increased repulsion as the value of U increases.

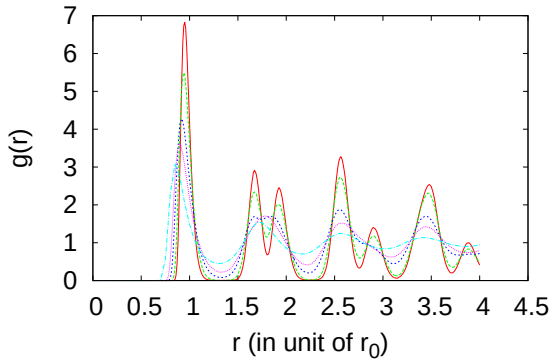

FIG. 7. (Color online) For a given interaction $U = 2$ eV, radial pair distribution function $g(r)$ for different temperatures: $T = 300$ K (full line), 600 K (thick dashed line), 1500 K (thin dashed line), 3000 K (dotted line), 6000 K (dotted-dashed line).

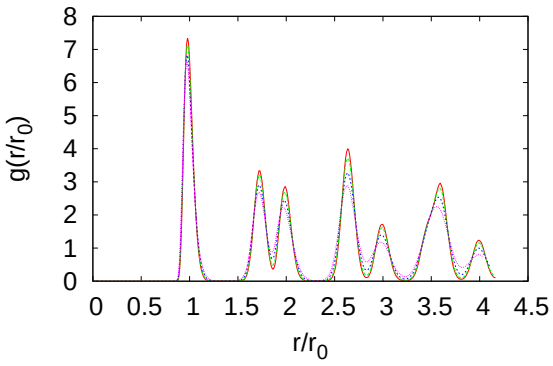

FIG. 8. (Color online) For a given temperature $T = 300$ K, radial pair distribution function $g(r/r_0)$ for different Coulomb interactions: $U = 0$ (full line), $U = 1$ eV (thick dashed line), $U = 2$ eV (thin dashed line), $U = 4$ eV (dotted line).

VI. SUMMARY AND CONCLUSION

We have derived for the first time a real-space version of the Gutzwiller method embedded into the MD simulations for strongly correlated electron systems. From a given set of atomic positions, a Hamiltonian can be constructed in terms of hopping integrals, on-site energies and Coulomb repulsion terms. It is precisely these interaction terms that require a treatment beyond mean-field HF-like theory, but can be described within the Gutzwiller method. This method is a variational method in the Rayleigh-Ritz sense, for which one minimizes the energy of the system via a set of local Gutzwiller variational parameter dependent on each site, thereby providing an approximate ground state energy for the system. This minimization can be computationally demanding, especially when all the sites are inequivalent. This has motivated the development of an accurate analytical

solution for finding the optimized double occupancy on each site.

MD simulation is a repeated two-step process. First, employing a Hellmann-Feynman theorem within the Gutzwiller ground state, we can calculate the quantum origin of the forces acting on the atoms. This ground state energy defines an interatomic potential, which explicitly accounts for correlation effects. Second, the atomic forces derived from this interatomic potential are input into the classical equations of motion and the atomic positions are updated in time for one time step using a numerical integrator (e.g., the Verlet algorithm). This process then continues.

A further approximation consists of avoiding exact diagonalization of the Hamiltonian from which, in principle, we can calculate the local DOS to obtain all necessary integrated quantities. Instead, we have proposed here to use the SMA, in which the true DOS is replaced by a rectangular constant DOS having the same second moment. Because the needed quantities to construct the variational ground state energy are basically integrated from DOS, they are less sensitive to the detailed structure of the DOS, thus validating the SMA. The second moment of the energy is easily computed from a few Hamiltonian matrix elements, where we can set up the MD process without invoking exact diagonalization to solve iteratively the Gutzwiller minimization. Therefore, a very accurate approximate, but analytical solution, is available, making this process feasible.

We concluded this first study with an application to a realistic case to show that this approach is promising. To our knowledge, this method has never been developed and will open up new possibilities for simulations of correlated electron materials with MD. We have applied the GA-MD method to the real-space lattice Anderson model. We have demonstrated the effect of temperature and electron correlation on structural properties simulated for the first time with MD. The generalization of these ideas to multiple correlated orbitals case is not made directly because of higher degeneracy. That is, the number of variational parameters increases as the number of atomic configurations (namely as 2^G, with G the degeneracy of the level) and therefore the number of local equations to be solved increases accordingly. We defer to future work on how to reduce the cost of calculating large number of variational parameters, and as in the single-correlated orbital model studied here, to find an analytical approach to the problem.

ACKNOWLEDGMENTS

We thank S. Valone, W. A. Harrison, and J. M. Wills for useful discussions. J.-P.J. would like to thank the Los Alamos National Laboratory for the hospitality and financial support during his visits. This work was carried out under the auspices of the National Nuclear Security Administration of the U.S. Department of Energy at LANL under Contract No. DE-AC52-06NA25396, and was supported by the LANL ASC Program. This work was in part supported by the LANL IMS Rapid Response Program and the Center for Integrated Nanotechnologies, a U.S. DOE user facility. Some preliminary results have been reported on the 2014 CECAM Workshop on Gutzwiller Wave Functions and Related Methods and documented in Ref. 21. A study of quantum MD to a single-band Hubbard model via exact diagonalization of the Gutzwiller variational Hamiltonian was recently reported in Ref. 24.

Appendix: Second moment approximation for bond quantities

To compute forces from the derivation of Hamiltonian, one needs average values like $\langle c_i^\dagger c_j \rangle$, with i and j being a short hand for site and spin-orbital states. Within these notations, and for the purpose of demonstration, we write the Hamiltonian H in simple tight-binding form:

$$H = \sum_{i \neq j} t_{ij} c_i^\dagger c_j + \sum_i \epsilon_i n_{i\sigma} \ , \tag{A.1}$$

where on-site energies $\epsilon_i = \langle i|H|i\rangle$ can be identified as average value of the Hamiltonian on local state labelled by i whereas hopping integrals $t_{ij} = \langle i|H|j\rangle$ couple states i to j. The bracket is the thermal average obtained for a general operator O by

$$\langle O \rangle = Tr \frac{e^{-\beta(H-\mu N)} O}{Z} \ , \tag{A.2}$$

where H, μ, N and Z are respectively the Hamiltonian, the chemical potential, the operator number of particles and the grand partition function. This average reduces to the ground state mean value at zero temperature. From exact diagonalization (as we do for the cluster example developed here), these quantities can easily be calculated from the weights $w(j,n)$ of state j (and similarly i) on eigenstate labelled by n and of energy ϵ_n:

$$\langle c_i^\dagger c_j \rangle = \sum_n f(\epsilon_n) w^*(i,n) w(j,n) \ , \tag{A.3}$$

where $f(\epsilon_n)$ is the Fermi distribution, from partial kinentic energy $e_i = \sum_j t_{ij} \langle c_i^\dagger c_j \rangle$ and partial occupancy $n_i = \langle c_i^\dagger c_i \rangle$ are obtained. This average reduces to the ground state mean value at zero temperature.

For large systems, where the speed of calculation is a limiting factor, it might be desirable however to avoid this diagonalization, and to find an approximate but cheap way to get them: that is precisely what the second moment approximation does.

The second moment approximation is based on the constraints that all necessary quantities are integrated quantities. Consequently, they are not sensitive to the fine details of the DOS, which will be replaced by rectangular DOS having the same second moment that the

true ones. The rectangular i-projected (centered on site energy ε_i with width W_i and height $1/W_i$) DOS has its second moment given by: $\varepsilon_i^2 + W_i^2/12$ whereas a direct path-counting (see Ref. 20) gives $\varepsilon_i^2 + \sum_{j\neq i} t_{ij}^2$. Identification between those two relations fixes uniquely the bandwidth W_i, from which the approximated i-projected DOS can be computed. This procedure has been widely used in semi-empirical molecular dynamics as in Ref. 18, for approximate local DOS. Within this approximation, the partial kinetic energy can be written as: $e_i = W_i n_i(n_i - 1)/2$.

All this can be straightforwardly extended to a multi-band case adding orbital index and spin to labels i and j. This procedure presents the great advantage of being very rapid compared to exact diagonalization.

[1] A. Georges, G. Kotliar, W. Krauth, and M. J. Rozenberg, Rev. Mod. Phys. **68**, 13 (1996).
[2] For a review, see G. Kotliar, S. Y. Savrasov, K. Haule, V. S. Oudovenko, O. Parcollet, C. A. Marianetti, Rev. Mod. Phys. **78**, 865 (2006).
[3] M.C. Gutzwiller, Phys. Rev. Lett. **10**, 159 (1963).
[4] M.C. Gutzwiller, Phys. Rev. **137**, A1726 (1965).
[5] J.-P. Julien and J. Bouchet, Prog. Theor. Chem. Phys., B 15, 509-534 (2006)
[6] D. Marx and J. Hutter *Ab Initio Molecular Dynamics. Basic Theory and Advanced Methods.* (Cambridge U. Press, Cambridge, UK, 2009).
[7] M. S. Daw and M. I. Baskes, Phys. Rev. B **29**, 6443 (1984).
[8] M. W. Finnis and J. E. Sinclair, Phil. Mag. A **50**, 45 (1984).
[9] M. I. Baskes, Phys. Rev. B **62**, 15332 (2000).
[10] T. Lee, M. I. Baskes, A. C. Lawson, S. P. Chen, and S. M. Valone, Materials **5**, 1040 (2012).
[11] J. Hubbard, Proc. Roy. Soc. London, **A 276**, 238 (1963).
[12] P. Nozières, *Magnétisme et localisation dans les liquides de Fermi*, Cours du Collège de France, Paris (1986).
[13] D. Vollhardt, Rev. Mod. Phys. **56**, 99 (1984).
[14] W.F. Brinkmann and T.M. Rice, Phys. Rev. B **2**, 1324 (1970).
[15] J.-X. Zhu, J.-P. Julien, Y. Dubi, and A. V. Balatsky, Phys. Rev. Lett. **108**, 186401 (2012).
[16] J. Friedel, Trans. Metall. Soc. AIME **230**, 616 (1964).
[17] W. A. Harrison, *Electronic Structure and the Properties of Solids* (W. H. Freeman and Co., San Francisco, 1980).
[18] G. J. Ackland and S. K. Reed, Phys. Rev. B **67**, 174108 (2003).
[19] M. S. Daw and M. I. Baskes, Phys. Rev. Lett. **50**, 1285 (1983).
[20] J.P. Gaspard and F. Cyrot-Lackmann, J. Phys. C: Solid State Phys. **6**, 3077 (1973).
[21] J. P. Julien, J. D. Kress and J.-X. Zhu, arXiv:1503.00933 (2015).
[22] D. Fincham, Computer Physics Communications **40**, 263 (1986).
[23] M.P. Allen and D.J. Tildesley, *Computer Simulation of Liquids* (Clarendon Press, Oxford, 1987).
[24] G.W. Chern, K. Barros, C. D. Batista, J. D. Kress, G. Kotliar, arXiv:1509.05860 (2015).